A Current-Tunable Sinusoidal Quadrature Oscillator Using Signal-Differencing All-Pass Filters

Banlue Srisuchinwong
Department of Electrical Engineering, Sirindhorn International Institute of Technology, Thammasat University, P.O.Box 22, Thammasat Rangsit Post Office, Patumthani 12121
email : banlue@siit.tu.ac.th

ABSTRACT – An integrable current-tunable sinusoidal quadrature oscillator is presented. A current-tunable all-pass filter is used as the frequency-selective network. The implementation is fully-balanced so as to enable accurate quadrature signals with symmetry. The osciilation frequency is current-tunable over a wide-freqency sweep range of approximately three orders of magnitude. The quadrature signals possess the amplitude matching and the quadrature phase matching of better than 0.004 dB and 0.15°, respectively. The maximum useful frequency of oscillation is in excess of 8 MHz, and total harmonic distortions can be adjusted easily to be approximately 0.5 percent.

KEY WORDS – Sinusoidal quadrature signals, current-tunable all-pass filters.

บทคัดย่อ – บทความนี้เสนอวงจรกำเนิดสัญญาณรูปซายน์แบบควอดราเจอร์ที่ปรับความถี่ด้วยการปรับค่าของกระแสไฟฟ้า โดยใช้วงจรกรองสัญญาณแบบออลพาสส์ที่ปรับค่ากระแสได้ วงจรมีความสมดุลเพื่อให้สัญญาณรูปซายน์มีความสมมาตร ความถี่ถูกปรับค่าได้ประมาณ 1,000 เท่าด้วยการปรับค่าของกระแส สัญญาณรูปซายน์แบบควอดราเจอร์ มีขนาดใกล้เคียงกันถึง 0.004 เดซิเบล และแตกต่างจากมุม 90 องศาไปน้อยกว่า 0.15 องศา ความถี่สูงสุดที่ใช้งานได้มีค่าสูงกว่า 8 เมกะเฮิรตซ์ ความเพี้ยนทางฮาร์โมนิกส์มีค่าประมาณ 0.5 เปอร์เซ็นต์

คำสำคัญ – สัญญาณรูปซายน์แบบควอดราเจอร์ วงจรกรองสัญญาณแบบออลพาสส์ที่ปรับค่ากระแสได้

1. Introduction

Quadrature oscillators typically provide two sinusoids with 90° phase difference for a variety of applications such as quadrature modulators and carrier recovery circuits. Integrable quadrature oscillators based on relaxation [1] and ring oscillators [2] have been reported. However, both types of oscillators are generally classified as nonlinear oscillators where periodically switching mechanisms are employed and therefore outputs may not be readily low-distortion sinusoidal waveforms [3]. Although two-integrator oscillators have also been suggested for integrable quadrature oscillators, they usually include some forms of relaxation [4, 5] or ring oscillators [6].

In constrast, linear oscillators employ frequency-selective networks such as LC or RC circuits and therefore low-distortion sinusoidal outputs can be readily generated [3,7]. Recently planar inductors [8], underetched coils [9] and bonding wire inductors [10] provide a good basis for integrable inductors, most LC oscillators are however difficult to tune over wide frequency ranges [7]. On the other hand, sinusoidal quadrature oscillators using RC all-pass filters have been the counterpart, but they usually require the use of operational amplifiers [11, 14]. Although current-mode RC all-pass filters and other current-mode approaches have been suggested for such oscillators [12, 15, 16], most of them require switching among different resistors (or capacitors) for a tunable frequency range. Techniques of a current-tunable bandpass filter have been reported for a wide-tunable frequency range and such switching is not necessarily needed [13].

In this paper, a new realisaton of an integrable current-tunable sinusoidal quadrature oscillator is presented using r_e tunable signal-differencing all-pass filters as the frequency-selective network, where r_e is the small-signal dynamic resistance of a

forward-biased based-emitter junction of a bipolar transistor. The implementation is fully-balanced so as to enable accurate quadrature signals with symmetry. The oscillation frequency is current-tunable over a wide-freqency sweep range of approximately three orders of magnitude. The quadrature signals possess the amplitude matching and the quadrature phase matching of better than 0.004 dB and 0.15°, respectively, and total harmonic distortions of approximately 0.5 percent. The maximum useful frequency of oscillation is in excess of 8 MHz.

2. Circuit Descriptions

Figure 1 shows the basic circuit configuration of the current-tunable sinusoidal quadrature oscillator consisting of two identical stages in series. Each stage is formed by a fully-balanced current-tunable all-pass filter connected with a differential amplifier. For the first stage, the all-pass filter is formed by ten matched transistors (Q1 to Q10), a capacitor C and two current sinks I and I_F, where the small-signal, differential, input voltage V_{AB} is applied to the bases of Q1 and Q2 between nodes A and B, and the small-signal, differential, output voltage V_{GF} is taken across the emitters of Q9 and Q10 between nodes G and F. The current I /2 biases the (Q3, Q9) and the (Q4, Q10) branches, whilst the frequency setting current I_F /2 biases the (Q1, Q8, Q7) and the (Q2, Q5, Q6) branches. The differential pair (Q21 and Q22), functioning as a voltage-to-current converter, constitutes the required loop gain controllable by the loop-gain setting current I_G to initiate and to sustain steady-stead oscillations.

Similarly, for the second stage, the all-pass filter is formed by ten matched transistors (Q11 to Q20), a capacitor C and two curent sinks I and I_F, where the small-signal, differential, input voltage V_{MN} is applied to the bases of Q11 and Q12 between nodes M and N, and the small-signal, differential, output voltage V_{OP} is taken across the emitters of Q19 and Q20 between nodes O and P. The current I /2 biases the (Q13, Q19) and the (Q14, Q20) branches, whilst the frequency setting current I_F /2 biases the (Q11, Q18, Q17) and the (Q12, Q15, Q16) branches. The differential pair (Q23 and Q24) constitutes the required loop gain controllable by the loop-gain setting current I_G to initiate and to sustain steady-stead oscillations.

It can be seen from Figure 1 that the input of the first stage V_{AB}, at nodes A and B, is connected to the output of the second stage, at nodes A′ and B′, but they possess the opposite polarities. On the other hand, at nodes M and N, the input of the second stage V_{MN} is connected to the output of the first stage, and they possess the same polarities. The circuit is fully-balanced so as to enable accurate quadrature signals with symmetry. The circuit is also relatively simple and integrable as devices can be fabricated on-chip.

3. Ideal Analysis

The analysis of Figure 1 assumes that each transistor acts as an idealised voltage-controlled current source (VCCS), where the collector current is simply equal to the small-signal voltage across the base-emitter nodes divided by r_e, where r_e is the usual ratio of the thermal voltage and the emitter bias current. The common-emitter current gain factors (β's) are also assumed to be infinite. As the two stages of Figure 1 are identical, only the first stage will be described. For clarity, the all-pass filter of the first stage can be isolated such that the inputs of the all-pass filter between nodes A and B are disconnected from the outputs of the second stage between nodes A′ and B′, and the outputs of the all-pass filter between nodes G and F are disconnected from the inputs of the differential amplifier between nodes G′ and F′.

For such isolation, it can be assumed for the moment that the bases of Q9 and Q10 at nodes D′ and E′ are temporarily disconnected from nodes D and E, respectively. As a result the bases of Q9 and Q10 at D′ and E′ are then temporarily connected together with an appropriate bias voltage say V_{bias}. In such temporary cases, let V_{O1} be the small-signal, differential, output voltage at node D with respect to node E, and V_{O2} be the small-signal, differential output voltage at node F with respect to node G. The input voltage V_{AB} results in a small-signal, differential, output current $i_{d1} = V_{AB} / 2r_{e1}$ passing, through nodes D and E, the loading impedance $4r_{e1} / (1+s\tau)$ where $r_{e1} = (2V_T / I_F)$ is the emitter resistance of either Q1, Q2, Q5, Q6, Q7 or Q8, V_T is the usual thermal voltage of approximately 25 mV associated with a pn junction at room temperature, and time constant $\tau = 4C\, r_{e1}$. Therefore the transfer function $V_{O1} / V_{AB} = 2 / (1+s\tau)$ represents a first-order low-pass filter. In addition, V_{AB} also results in another small-signal, differential, output current $i_{d2} = V_{AB} / 2r_{e2}$ passing, through nodes F and G, the loading resistance $2r_{e2}$ where $r_{e2} = (2V_T / I)$ is the emitter resistance of either Q3, Q4, Q9 or Q10. Therefore the transfer function $V_{O2} / V_{AB} = 1$ represents a buffer.

By reconnecting the bases of Q9 and Q10 at nodes

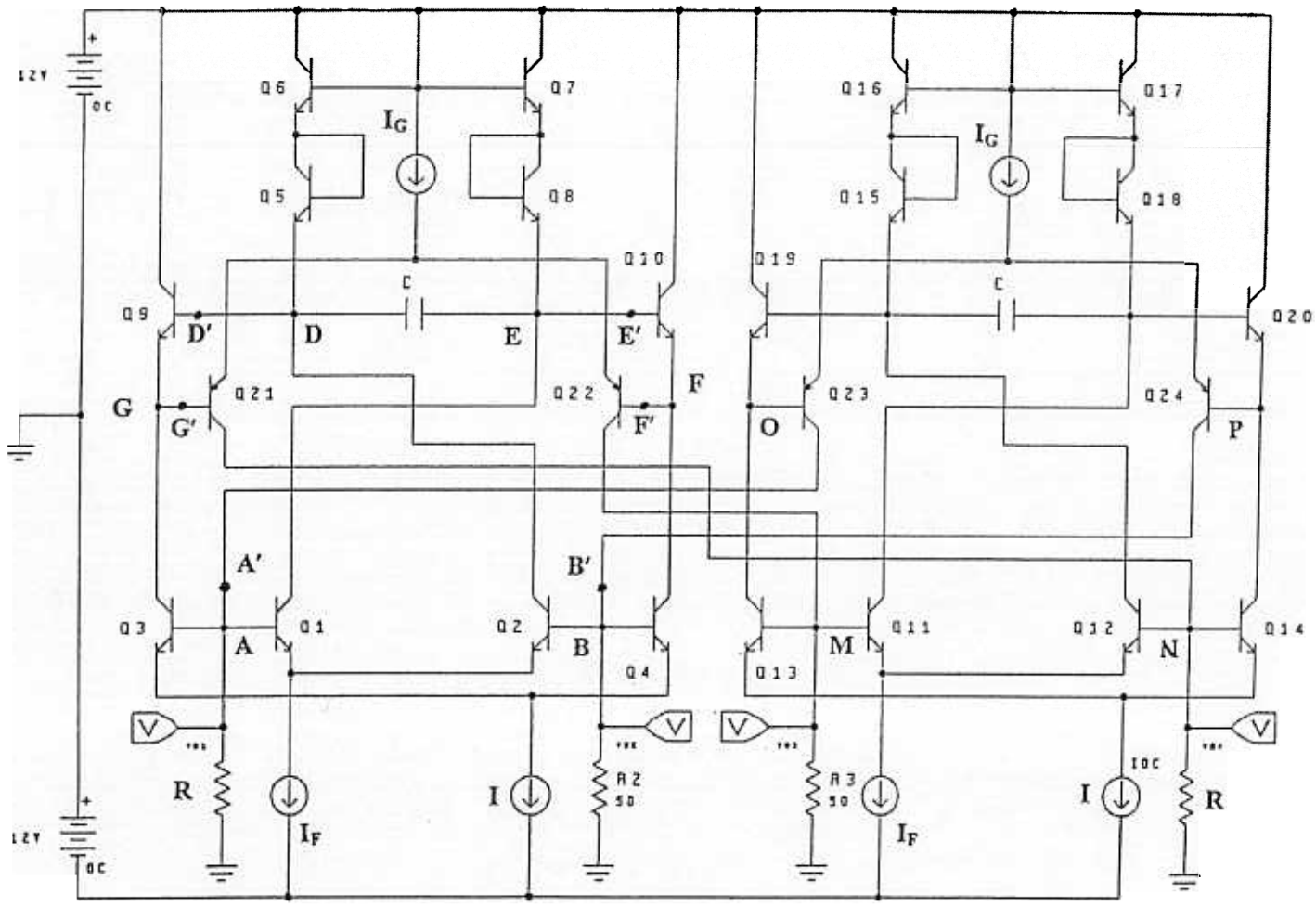

Figure 1 : Circuit diagram of the fully-balanced current-tunable sinusoidal quadrature oscillator.

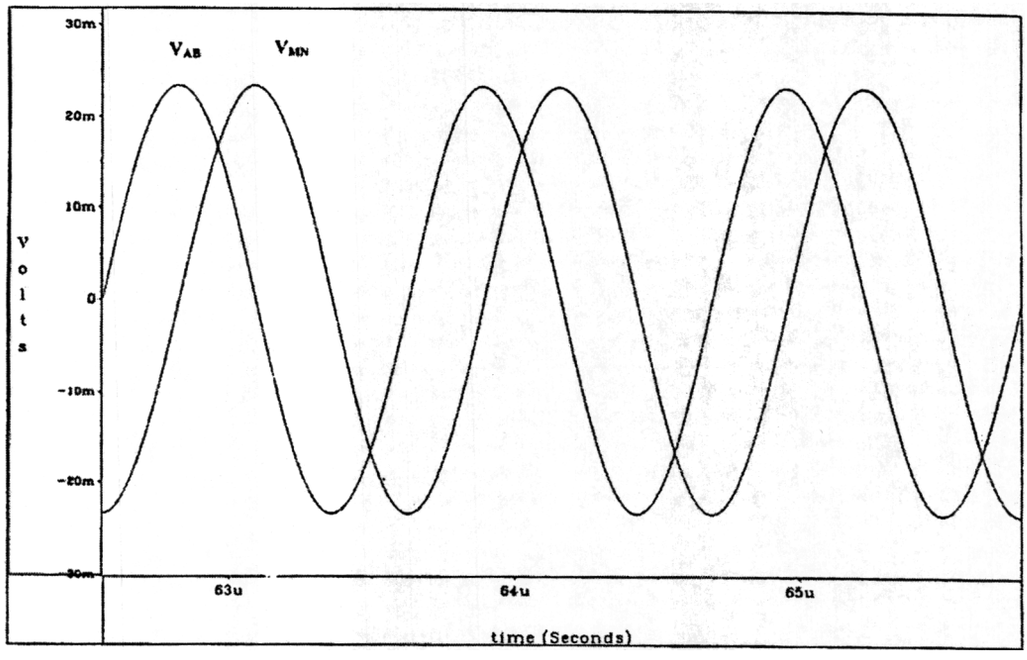

Figure 2 : Oscillograms of the quadratrue waveforms V_{AB} and V_{MN} at $I_F / 2$ = 700 uA.

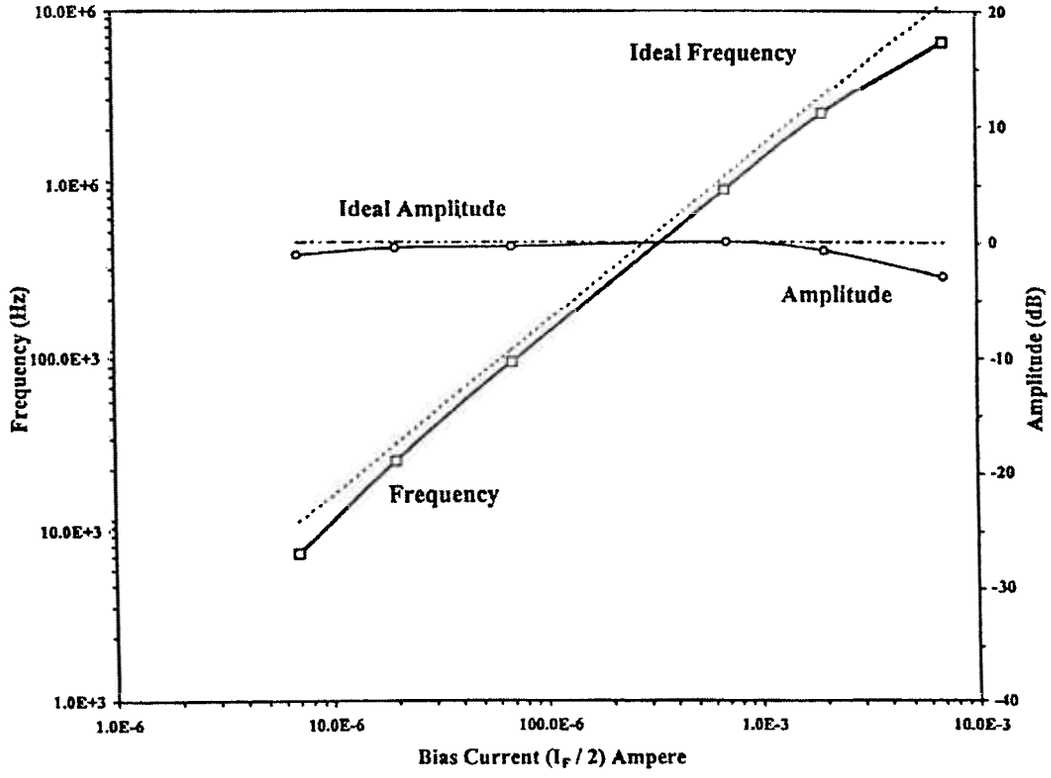

Figure 3 : Plots of oscillation frequencies and amplitude versus bias currents $I_F / 2$.

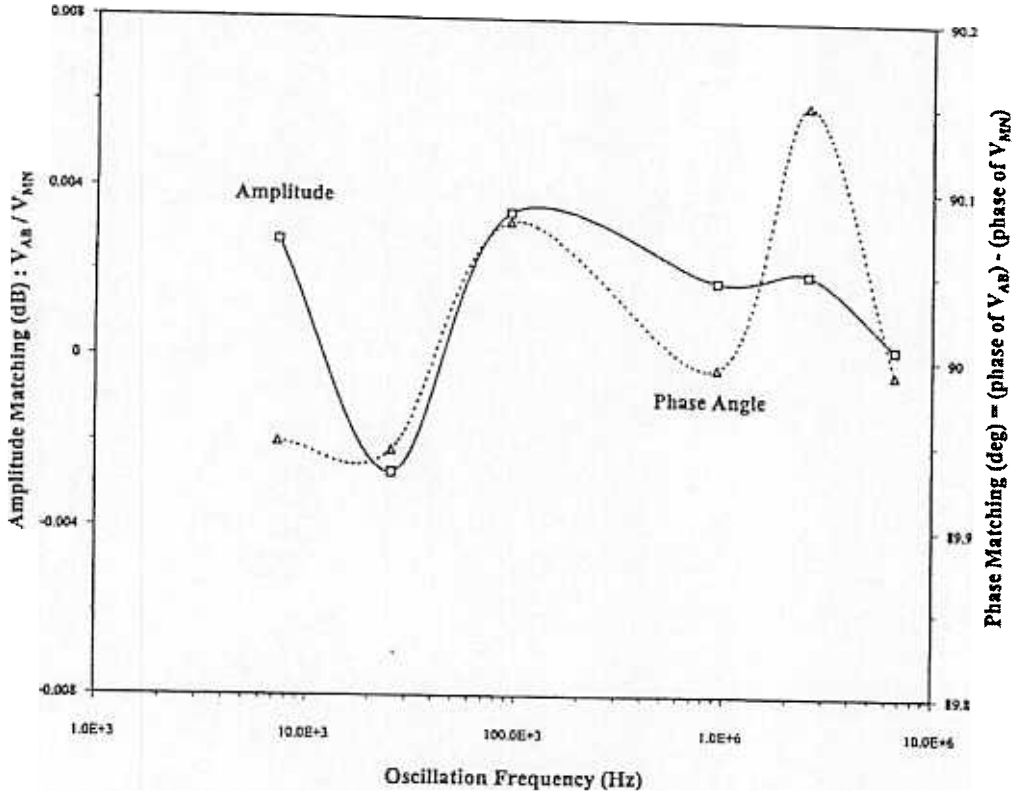

Figure 4 : Amplitude and phase matching of the quadrature signals versus frequency.

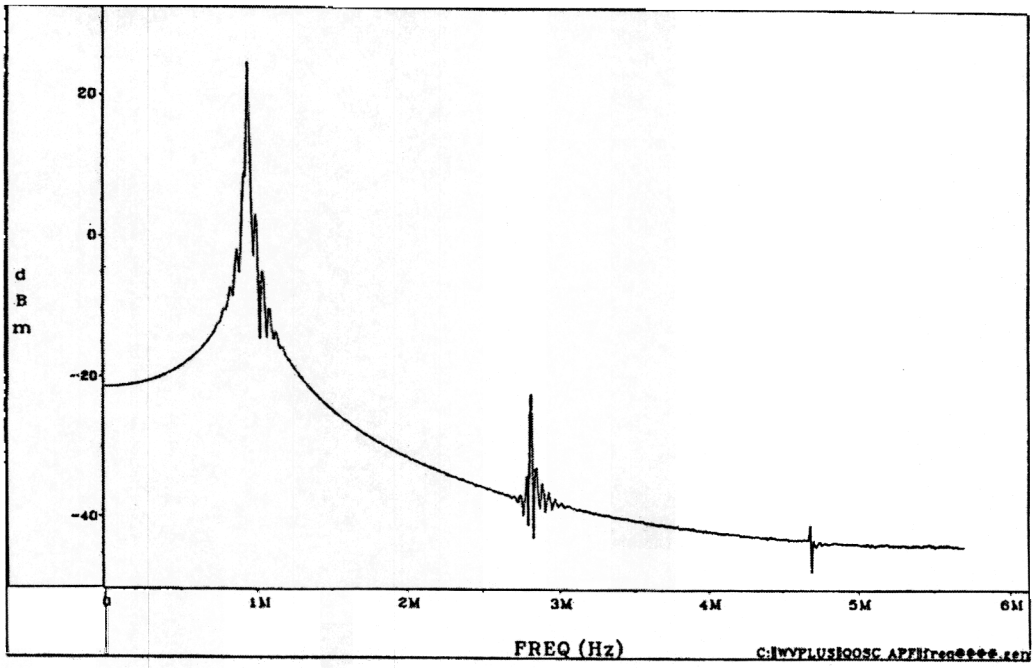

Figure 5 : Harmonic spectrums of the output waveform V_{AB} at $I_F/2$ = 700 uA.

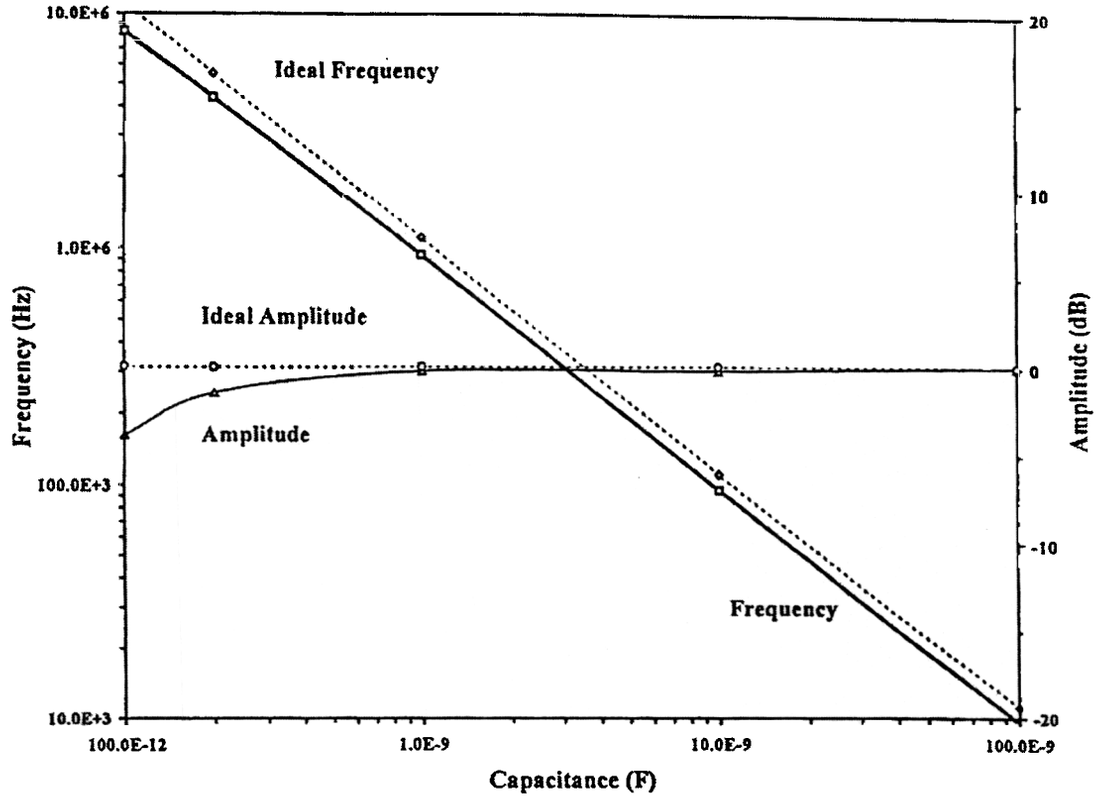

Figure 6 : Plots of oscillation frequencies and amplitude versus frequency setting capacitances.

D′ and E′ with nodes D and E, respectively (as shown in Figure 1), the total output voltage V_{GF}, at node G with respect to node F, is obtained through superposition, i.e. $V_{GF} = V_{O1} - V_{O2}$ and hence the name "Signal Differencing". Consequently, the transfer function V_{GF} / V_{AB} represents an all-pass filter with phase angle θ of the forms

$$\frac{V_{GF}}{V_{AB}} = \frac{1 - s\tau}{1 + s\tau} \qquad (1)$$

$$\theta = -2 \tan^{-1} (\omega\tau) \qquad (2)$$

where $\theta = -\pi/2$ at $\omega = 1/\tau = I_F / (8CV_T)$.

As mentioned earlier, V_{AB} between nodes A and B and the resulting small-signal, differential, output voltage $V_{A'B'}$ between nodes A′ and B′ possess the opposite polarities. Therefore it can be shown that the relationship between V_{AB} and $V_{A'B'}$ can be written as

$$\frac{V_{A'B'}}{V_{AB}} = -\left[G\left(\frac{1 - s\tau}{1 + s\tau}\right)\right]^2 \qquad (3)$$

where $G = R / r_{e3}$ and $r_{e3} = (2V_T / I_G)$ is the emitter resistance of either Q21 or Q22 of the first stage, or either Q23 or Q24 of the second stage. For steady-state sinusoidal oscillations to be sustained, the ratio $V_{A'B'} / V_{AB}$ must be unity. Therefore, upon setting (3) to unity and rearranging, one obtains

$$s^2 + s\frac{2}{\tau}\left(\frac{1 - G^2}{1 + G^2}\right) + \frac{1}{\tau^2} = 0 \qquad (4)$$

Upon substituting s in (4) with $j\omega_0$, and setting the real and the complex parts to zero

simultaneously, the required value of G to sustain steady-state sinusoidal oscillations and the angular frequency of oscillations ω_0 can be written as

$$G = \frac{R}{r_{e3}} = R\frac{I_G}{\quad} = 1 \qquad (5)$$

$$\omega_0 = \frac{1}{\tau} = \frac{}{8CV_T} \qquad (6)$$

It can be seen from (5) that the required condition for steady-state oscillations can be set by adjustments of I_G. It can be seen from (6) that the frequencies of oscillations are linearly proportional to the bias current I_F and hence the name "Current-Tunable". At the oscillation frequency ω_0, as suggested by (2), the phase angle θ_0 of V_{MN} of the second stage is different from the phase angle θ_1 of V_{AB} of the first stage by $\theta_0 - \theta_1 = -\pi/2$. In order words, V_{MN} and V_{AB} provide quadrature oscillation of values sin θ_0 and cos θ_0, respectively, and hence the name "Sinusoidal Quadrature Oscillator".

4. Simulation Results

The performance of the circuit shown in Figure 1 has been simulated through SPICE. The npn and pnp transistors are modeled by QMPS2222A and QMP3640, where the average transition frequencies (f_T) are at 300 and 500 MHz, repectively. As an example, the values of capacitor C is equal to 1000 pF, bias current I and I_G are approximately 200 uA and 1.2 mA, respectively, and R = 50 Ω. Figure 2 shows the resulting oscillograms of the quadrature waveforms V_{AB} and V_{MN} at, for example, $I_F / 2$ = 700 μA where the oscillation frequency is measured to be 936 kHz. It can be seen from Figure 2 that V_{AB} and V_{MN} are, as suggested previously, cosine and sine signals, respectively, with 90° phase difference. Figure 3 illustrates comparisons of the plots of oscillation frequencies and amplitudes versus bias current I_F / 2 for cases of ideal analysis and SPICE analysis. It can be seen from Figure 3 that the oscillation frequencies are, as suggested by (6), tunable by the bias current I_F over approximately three orders of magnitude.

Figure 4 depicts the amplitude matching (dB) in terms of the ratio V_{AB}/V_{MN}, as well as the phase matching (deg) in terms of [(phase of V_{AB}) – (phase of V_{MN})] of the quadrature signals versus frequency. It is evident from Figure 4 that the amplitude matchin is 0.004 dB, whilst the phase matching for 90° is better than 0.15°. Figure 5 shows the power levels (dBm) of the fundamental frequency and the next harmonics of the oscillogram V_{AB} depicted in Figure 2 using commercially available fast Fourier transform (FFT) program. It is clearly seen from Figure 5 that distortions are due mainly to the presence of the third harmonics which is approximately 47 dBm down from the fundamental frequency, and they remain essentially at the same magnitude over the entire operational bias-current range (7 μA to 7 mA). The measured total harmonic distortions (THD) of the output waveforms, as shown in Figure 5, are less than 0.5 percent.

Figure 6 illustrates comparisons of the plots of oscillation frequencies and amplitudes versus capacitances, for cases of ideal theory and the SPICE simulated results, and the bias current I_F / 2 is fixed at 700 μA. It is seen that, using a minimum frequency setting capacitances of 100 pF, the upper frequency can be expected at 8 MHz.

5. Discussion and Conclusions

A new fully-balanced current-tunable sinusoidal quadrature oscillator has been presented using r_e tunable signal-differencing all-pass filters as the frequency-selective network. The oscillation frequency is current-tunable over a wide-freqency sweep range of approximately three orders of magnitude. The amplitude matching and the quadrature phase matching are better than 0.004 dB and 0.15°, respectively. The total harmonic distortions are approximately 0.5 percent. The maximum useful frequency of oscillation is approximately 8 MHz. By using better transistors of much higher f_T (e.g. in the region of several GHz) and much smaller value of C (e.g. using stray capacitance), much higher, more useful, values of the oscillation frequency, as suggested by (6), may be expected.

Acknowledgements

The author is grateful to M. Watchakittikorn for his useful suggestion.

References

[1] C.J.M. Verhoeven, "A high-frequency electronically tunable quadrature oscillator",

IEEE Journal of Solid-State Circuits, Vol.27, 1992, pp. 1097-1100.

[2] A.W. Buchwald, and K.W. Martin, "High-speed voltage-controlled oscillator with quadrature outputs, *Electronics Letters*, 27, 1991, pp. 309-310.

[3] D. A. Johns and K. Martin, *Analog Integrated Circuit Design*, John Wiley & Sons, 1997.

[4] J. Davidse, *Analog Electronic Circuit Design*, Prentice Hall, 1991.

[5] B. Linares-Barranco, A. Rodrigez-Vazquez, E. Sanchez-Sinencio, J.L. Huertas, "10 Mhz CMOS OTA-C voltage-controlled quadrature oscillator", *Electronics Letters*, vol. 25, 1989, pp. 765-767.

[6] J.van der Tang, D. Kasperkovitz, "A 0.9-2.2 Ghz monolithic quadrature mixer oscillator for direct-conversion satellite receivers", *Proceedings of the 1997 IEEE International Solid-State Circuits Conference*, February, 1997, 40, pp. 88-89.

[7] A. Sedra and K.C. Smith, *Microelectronic Circuits*, 4th Ed., Oxford University Press, 1998.

[8] R. Duncan, K. Martin, A. Sedra, "1 Ghz quadrature sinusoidal oscillator", *Proceedings of the 1995 17th Annual Custom Integrated Circuits Conference*, May, 1995, pp. 91-94.

[9] A. Rofougaran, J. Rael, M. Rofougaran, and A. Abidi, "A 900 Mhz CMOS LC-oscillator with quadrature outputs", *Proceedings of the 1996 IEEE International Solid-State Circuits Conference*, Vol. 39, 1996, pp. 392-393.

[10] J. Craninckx, and M. Steyaert, "A CMOS 1.8 Ghz low-phase-noise voltage-controlled oscillator with prescaler", *Proceedings of the 1995 IEEE International Solid-State Circuits Conference*, Vol. 38, 1995, 266-267.

[11] S. Pookaiyaudom and K. Saivichit, "RC phase-shifter variable sinusoidal oscillators using initial conditions-restoration amplitude control", *IEEE Transactions on Instrumentation and Measurement*, Vol. 39, 1990, pp. 1038-1044.

[12] S. Pookaiyaudom and K. Samootrut, " Current-mirror phase-shifter oscillator", *Electronics Letters*, Vol. 23, 1987, pp. 21-23.

[13] S. Pookaiyaudom, B. Srisuchinwong, and W. Kurutach, "A current-tunable sinusoidal oscillator", *IEEE Transactions on Instrumentation and Measurement*, Vol. IM-36, No. 3, 1987, pp. 725-729.

[14] R. Holzel, "A simple wide-band sine wave quadrature oscillator", *IEEE Transactions on Instrumentation and Measurement*, Vol. 42, 1993, pp. 758-760.

[15] J.J. Chen, C.C Chen, H.W. Tsao and S.I. Liu, "Current-mode oscillators using single current follower", *Electronics Letters*, Vol. 27, 1991, pp. 2056-2058.

[16] S.I. Liu and Y.H. Liao, "Current-mode quadrature sinusoidal oscillator using FTFN", *International Journal of Electronics*, Vol. 81, 1996, pp.171-175.